Proc. Natl. Acad. Sci. USA
Vol. 88, pp. 6873–6877, August 1991
Biophysics

Replacement of leucine-93 by alanine or threonine slows down the decay of the N and O intermediates in the photocycle of bacteriorhodopsin: Implications for proton uptake and 13-*cis*-retinal → all-*trans*-retinal reisomerization

(integral membrane protein/proton pump/site-specific mutagenesis/conformational change/resonance Raman spectroscopy)

SRIRAM SUBRAMANIAM*, DUNCAN A. GREENHALGH*, PARSHURAM RATH†, KENNETH J. ROTHSCHILD†, AND H. GOBIND KHORANA*

*Departments of Biology and Chemistry, Massachusetts Institute of Technology, 77 Massachusetts Avenue, Cambridge, MA 02139; and †Department of Physics, Physiology and Program in Cellular Biophysics, Boston University, Boston, MA 02215

Contributed by H. Gobind Khorana, April 23, 1991

ABSTRACT **We report that the replacement of Leu-93 in bacteriorhodopsin by Ala (L93A) or Thr (L93T) slows down the photocycle by ≈100-fold relative to wild-type bacteriorhodopsin. Time-resolved visible absorption spectroscopy and resonance Raman experiments, respectively, show the presence of long-lived O-like and N-like intermediates in the photocycles of the above mutants. We infer the existence of an equilibrium between the N and O intermediates in the photocycles of these mutants. The L93A and L93T mutants exhibit normal proton pumping under continuous illumination, suggesting that the decay of the N and/or O intermediate, and consequently, proton translocation, can be accelerated by the absorption of a second photon. Since the 13-cis → all-trans reisomerization of retinal is completed during the decay of the N and O intermediates, we conclude that the interaction of Leu-93 with retinal is important in this phase of the photocycle. This conclusion is supported by a recent structural model of bacteriorhodopsin that suggests that Leu-93 is near the C-13 methyl group of retinal.**

Bacteriorhodopsin (bR), a retinal-based membrane protein in the extreme halophile *Halobacterium halobium*, is a light-driven proton pump (1). Proton transport is initiated by the light-induced, all-trans → 13-cis isomerization of retinal. This results in a series of cyclic changes in protein conformation reflected by the formation and decay of at least five distinct photointermediates: K, L, M, N, and O. A proton is released into the extracellular medium during the formation of the M intermediate (2), and a proton is taken up from the cytoplasm during the decay of the N intermediate (3–5). Site-specific mutagenesis studies of bR, in combination with a variety of spectroscopic methods, have demonstrated the participation of Asp-85, Arg-82, and Asp-212 in proton release and of Asp-96 in proton uptake during the photocycle (6–12).

Mutagenesis studies have also indicated that a number of amino acids appear to interact with retinal. Amino acid replacements of Thr-89, Ser-141, or Tyr-185 alter the visible absorption spectrum and allow the formation of multiple cis isomers of retinal upon illumination (13, 14). Mutants in which Trp-86, Trp-182, Pro-186, or Trp-189 have been replaced display blue-shifted absorption maxima, indicating proximity to retinal (15). The above residues are among a group of 21 amino acids that have been proposed to constitute the retinal binding pocket in bR (16).

The light-driven all-trans → 13-cis isomerization of retinal early in the photocycle is reversed during the decay of the N intermediate (17). Both isomerization steps are generally believed to be associated with changes in protein conformation. To understand how changes in retinal geometry are coupled to conformational changes in the protein, we are carrying out systematic replacements of amino acids that line the retinal binding pocket. We report here that the interaction of Leu-93, a residue in helix C (Fig. 1), with retinal has an important role in the photocycle and in light/dark adaptation. Time-resolved visible spectroscopic studies show that the half-time for the decay of the O intermediate of the photocycle is increased to ≈800 ms in the mutants where Leu-93 was replaced by Ala (L93A) or Thr (L93T) as compared to a rate of <5 ms for wild-type bR. Resonance Raman (RR) experiments provide evidence for the presence of a long-lived N intermediate in the photocycles of these mutants. We conclude that Leu-93 in bR is involved in coupling protein conformational changes that occur during the decay of the N and O intermediates of the photocycle to 13-cis → all-trans reisomerization of the chromophore.

MATERIALS AND METHODS

Construction and Purification of Mutant Proteins. The mutants L93A, L93T, and L93V were constructed in a synthetic bacterioopsin gene, expressed in *Escherichia coli*, and purified using previously described methods (6). Chromophores were formed by the addition of either 13-*cis*- or all-*trans*-retinal to an equimolar amount of the corresponding apoprotein in 1% dimyristoyl phosphatidylcholine/1% 3-[(3-cholamidopropyl)dimethylammonio]-1-propanesulfonate/0.2% SDS/50 mM sodium phosphate at pH 6.0. For the time-resolved photocycle and RR measurements, dodecyl sulfate was removed as the insoluble potassium salt by the addition of KCl to a final concentration of 150 mM. Dark-adapted spectra were recorded after storage of the protein in the dark for at least 48 hr at 4°C. Light adaptation was carried out by illumination for 3 min with a 100-W fiber optic illuminator (Oriel, Stamford, CT) equipped with a 495-nm cutoff filter (Melles Griot, Irvine, CA). The retinal isomer composition in the mutants was determined as described in ref. 13.

Steady-State Proton Pumping Measurements. Proton-pumping assays were carried out on protein samples that were reconstituted into soybean lipid vesicles by detergent dilution (6).

The publication costs of this article were defrayed in part by page charge payment. This article must therefore be hereby marked "*advertisement*" in accordance with 18 U.S.C. §1734 solely to indicate this fact.

Abbreviations: bR, bacteriorhodopsin; RR, resonance Raman. bR mutants are designated by the wild-type amino acid residue (single-letter code) and its sequence number followed by the substituting amino acid residue. For example, in the mutant L93A, Leu-93 is replaced by Ala.

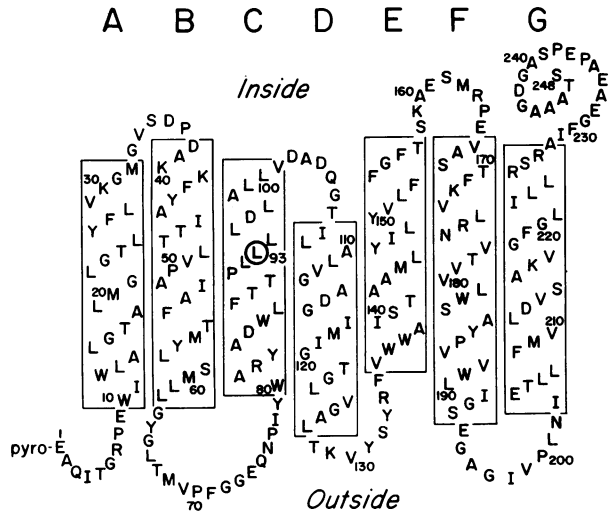

FIG. 1. Secondary structure model of bR according to Henderson *et al.* (16). Leu-93 is circled.

Visible and RR Spectroscopic Studies of Photocycle Intermediates. Time-resolved measurements of the photocycle by visible spectroscopy were carried out as described (14). RR spectra (resolution ≈ 5 cm^{-1}) of wild-type bR and the L93A and L93T mutants were obtained by exciting the samples in a spinning quartz cell (18) with the cylindrically focused 514.5-nm beam (3 mW) of an argon ion laser (Coherent Radiation, Palo Alto, CA). The time period for one complete rotation of the sample cell was about 22 ms, and the transit time through the beam was ≈ 10 μs. For the pulsed RR spectrum of the L93A mutant, the sample was illuminated for a period of 100 ms every 2 s, in order to allow complete decay of the long-lived intermediates. Identical samples were used for the RR and the visible spectroscopic experiments.

RESULTS

Renaturation and Chromophore Formation in the Leu-93 Mutants with 13-*cis*- or all-*trans*-retinal. The properties of the chromophores formed upon the addition of either all-*trans*- or 13-*cis*-retinal to wild-type and mutant bacterioopsin are summarized in Table 1. Addition of 13-*cis*- or all-*trans*-retinal to wild-type bacterioopsin in mixed micelles results in the formation of chromophores with absorption maxima (λ_{max}) at 542 nm and 558 nm, respectively. In contrast, the chromophores generated in the L93A mutant with either 13-*cis*- or all-*trans*-retinal have a λ_{max} at 531 nm. A similar result was obtained for the L93T mutant (Table 1). The λ_{max} values for the L93V mutant are 554 nm and 544 nm when the chromophores are formed with all-*trans*- or 13-*cis*-retinal, respectively. In each case, the samples regenerated with either 13-*cis*- or all-*trans*-retinal display the same final dark-adapted absorption spectrum (Table 2) after storage in the dark for 48 hr.

Table 1. Kinetics of chromophore formation at 20°C with 13-*cis*- or all-*trans*-retinal in dimyristoyl phosphatidylcholine/3-[(3-cholamidopropyl)dimethylammonio]-1-propanesulfonate mixed micelles at pH 6 for wild-type bR and the mutants

Sample	13-*cis*-retinal		all-*trans*-retinal	
	$t_{1/2}$, min	λ_{max},* nm	$t_{1/2}$, min	λ_{max},* nm
Wild type	2.0	542	2.2	558
L93A	10.2	531	2.0	531
L93T	8.7	531	1.3	529
L93V	3.3	544	1.9	554

*λ_{max} values are from absorption spectra recorded 10 min after the addition of retinal to the apoprotein.

In contrast with wild-type bR, a common feature of all the Leu-93 mutants is that the rates of chromophore formation are significantly slower with 13-*cis*-retinal than with all-*trans*-retinal (Table 1). For the L93A mutant, half-times of 2.0 and 10.2 min are observed for chromophore regeneration with all-*trans*- and 13-*cis*-retinal, respectively. The corresponding times for the L93T mutant are 1.3 and 8.7 min, and those for the L93V mutant are 1.9 and 3.3 min, respectively. The relatively minor effect of the Leu-93 → Val replacement on the kinetics of chromophore regeneration and the λ_{max} suggest that the requirements at residue 93 are probably for a large hydrophobic residue. The above observations indicate that Leu-93 is an important structural component of the retinal binding pocket.

Effect of Leu-93 Replacements on Retinal Isomer Composition. Illumination of dark-adapted wild-type bR with yellow light shifts the λ_{max} of the spectrum from 551 nm to 559 nm, with an increase in the extinction coefficient at the absorption maximum (Fig. 2 and Table 2). These effects of light adaptation are due to a shift in the isomer composition in favor of all-*trans*-retinal (1). In contrast, the dark- and light-adapted spectra of the L93A and L93T mutants are very similar, with λ_{max} values of 532 and 531 nm, respectively. In the L93V mutant, light adaptation shifts the λ_{max} from 547 nm to 553 nm, but this is accompanied by a decrease in the extinction coefficient at the absorption maximum and the appearance of an additional blue-shifted species with a λ_{max} at $\approx$430 nm.

Under the conditions of our experiment, the light-adapted form of wild-type bR predominantly contains the all-trans isomer (94%) with a minor amount (6%) of the 13-cis isomer. In the dark-adapted state, the all-trans to 13-cis isomer ratio is 42:58 (Table 2). In the L93A and L93T mutants, the dark-adapted forms of the chromophore contain $\approx$80% of the all-trans isomer and $\approx$20% of the 13-cis isomer. Only a small change in the isomer composition is observed upon light adaption (Table 2). These results show that in these mutants, the retinal binding pocket preferentially accommodates the all-trans isomer in both dark- and light-adapted states. The presence of similar retinal isomer ratios in the dark- and light-adapted forms is consistent with the observation that there is little change in the absorption spectrum upon light/dark adaptation. The retinal isomer composition of L93V in the dark-adapted form is closer to that of wild-type bR than to that of the L93A and L93T mutants. The light-adapted form contains predominantly all-*trans*-retinal (83%), but significant amounts of cis isomers can be detected (Table 2).

Time-Resolved Photocycle Studies of Wild-Type bR and the Leu-93 Mutants. Fig. 3 shows the difference spectra derived from time-resolved visible absorption measurements of the photocycle of wild-type bR at pH 6. The kinetic parameters of the photocycle of wild-type bR are in agreement with the earlier work of Otto *et al.* (9). The kinetics for M formation are biphasic with fast ($\approx$1 μs) and slow ($\approx$10 μs) components. The M intermediate decays back to the ground state with a $t_{1/2}$ of about 2.5 ms. The λ_{max} of the M intermediate is blue-shifted by $\approx$10 nm in the later time points. A similar observation has been reported for the photocycle of detergent-solubilized purple membrane (19).

The early stages of the photocycle of the L93A mutant (Fig. 4) are similar to that of wild-type bR. The kinetics for M formation match well with the slow component seen in the corresponding step of the wild-type photocycle. There is, however, a striking difference in the latter part of the photocycle. The decay of the M intermediate results in the accumulation of a red-shifted intermediate that has a λ_{max} at $\approx$595 nm in the difference spectrum. The half-time for the decay of this intermediate is about 800 ms. Since the λ_{max} of this intermediate is considerably red-shifted with respect to

Table 2. Retinal isomer composition for wild-type bR and the mutants in the dark- and light-adapted states at pH 6

	Dark-adapted			Light-adapted			
Sample	λ_{max}, nm	% all-trans	% 13-cis	λ_{max}, nm	% all-trans	% 13-cis	% other cis*
Wild-type	551	42	58	559	94	6	—
L93A	532	79	21	532	86	14	—
L93T	531	78	22	531	84	16	—
L93V	547	27	73	553	83	6	11

*Contributions from 11-cis, 9-cis, and di-cis isomers.

the λ_{max} of the ground state, we conclude that this is similar to the O intermediate of the wild-type photocycle.

To exclude the possibility that the long-lived O intermediate is due to an artifact of the micellar system, the photocycle of the L93A mutant was also studied in reconstituted vesicles containing *H. halobium* lipids. Between pH 5 and 8.5, the rate of decay of the O intermediate is essentially unchanged with a $t_{1/2}$ of ≈500 ms (unpublished observations).

The photocycle of the L93T mutant is similar to that of the L93A mutant (Table 1). In the L93V mutant, the sequence and kinetics of the intermediates observed during the decay of the M intermediate are similar to those of wild-type bR. However, both the rate of decay of the K intermediate and the rate of formation of the M intermediate are accelerated ($t_{1/2}$ < 300 ns).

Identification of a Long-Lived N Intermediate in the Photocycles of the L93A Mutant by RR Spectroscopy. The visible time-resolved difference spectra (Fig. 4) provide evidence for a long-lived O intermediate in the L93A photocycle. The presence of an N intermediate in the photocycle is more difficult to determine from examining the difference spectra, since the λ_{max} of the N intermediate is expected to be close to that of the ground-state chromophore. We have therefore used RR spectroscopy to investigate structural changes in the chromophore during the late stages of the photocycle of the L93A mutant.

Fig. 5*A* displays the RR spectrum of light-adapted wild-type bR. Contributions from all photointermediates are minimized because of the low photoalteration rate (laser power ≈3 mW) and the utilization of a spinning cell whose rotation time (22 ms) is greater than the photocycle period of wild-type bR. The RR spectrum of the L93A mutant (Fig. 5*B*) shows two noticeable differences from the wild-type bR spectrum: (*i*) The band due to the ethylenic stretch mode of the L93A chromophore is at 1536 cm^{-1} as compared to 1529 cm^{-1} for wild-type bR. This shift is expected from the blue-shifted λ_{max} of the mutant and the approximately linear correlation that exists between the frequency of this mode and the λ_{max} of the retinylidene chromophore (21). (*ii*) There is an intensified shoulder near 1186 cm^{-1} in the mutant spectrum, which is also seen in the RR spectrum of the L and N intermediates of wild-type bR and is due to a C — C stretch mode of the 13-cis form of the chromophore (17, 18).

To determine whether the spinning-cell RR spectrum of the L93A mutant contains contributions from a long-lived intermediate in the photocycle, the RR spectrum was recorded by

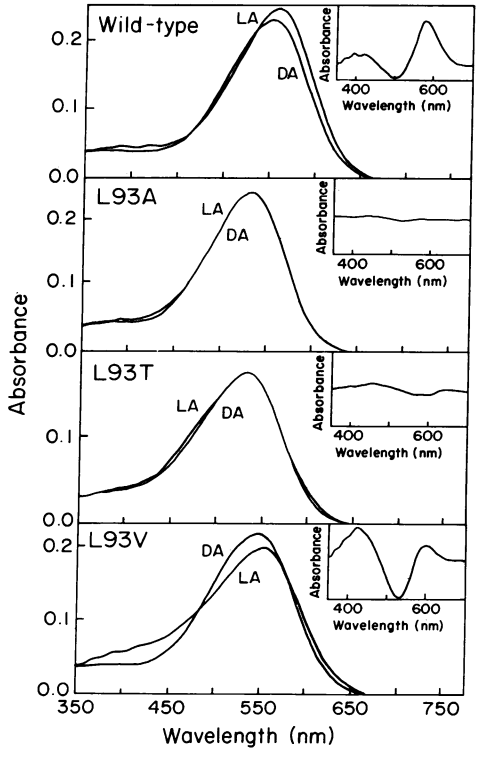

FIG. 2. Dark-adapted (DA) and light-adapted (LA) visible absorption spectra of wild-type bR, and the mutants L93A, L93T, and L93V in mixed micelles. (*Insets*) Five-fold magnification of the difference between the light- and dark-adapted absorption spectra.

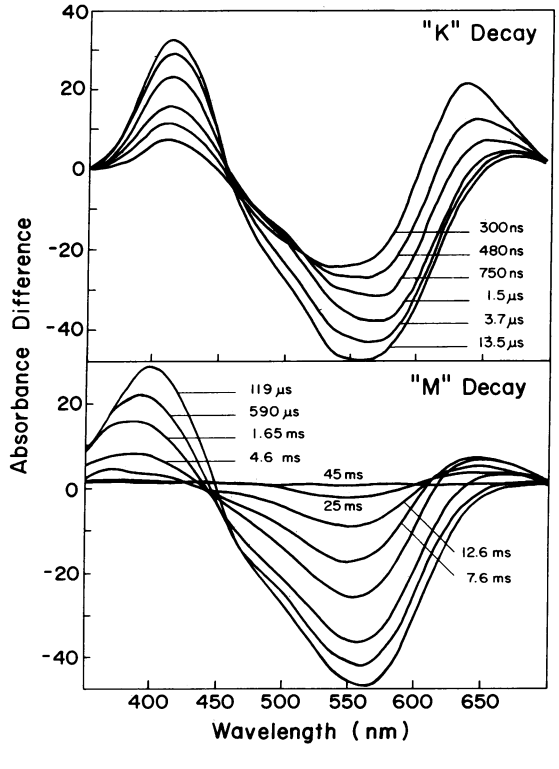

FIG. 3. Time-resolved difference spectra of intermediates in the photocycle of wild-type bR in mixed micelles at pH 6.0. (*Upper*) Spectral changes during the rise of the M photointermediate. (*Lower*) Decay of the M intermediate to bR via the formation and decay of the O intermediate. Each difference spectrum reflects the average of 300 acquisitions.

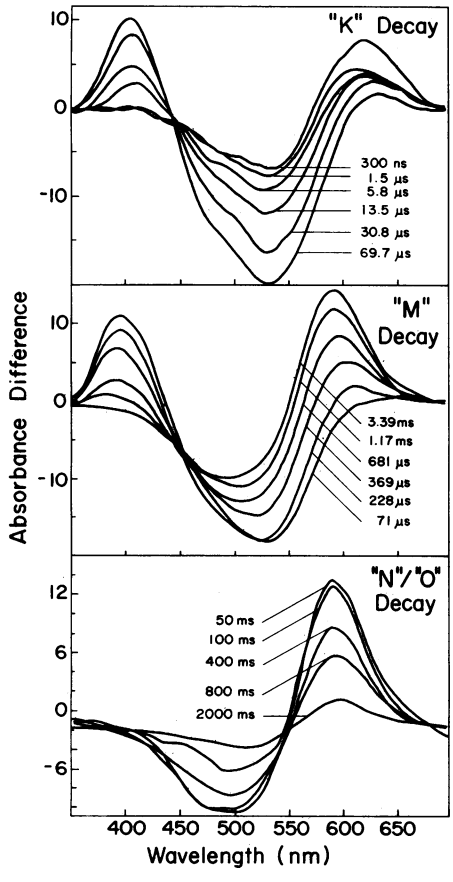

FIG. 4. Time-resolved difference spectra of intermediates in the photocycle of the mutant L93A in mixed micelles at pH 6.0. (*Top*) Spectral changes during the rise of the M photointermediate. (*Middle*) Decay of the M intermediate to an O-like intermediate. (*Bottom*) Slow decay of the O-like intermediate to bR.

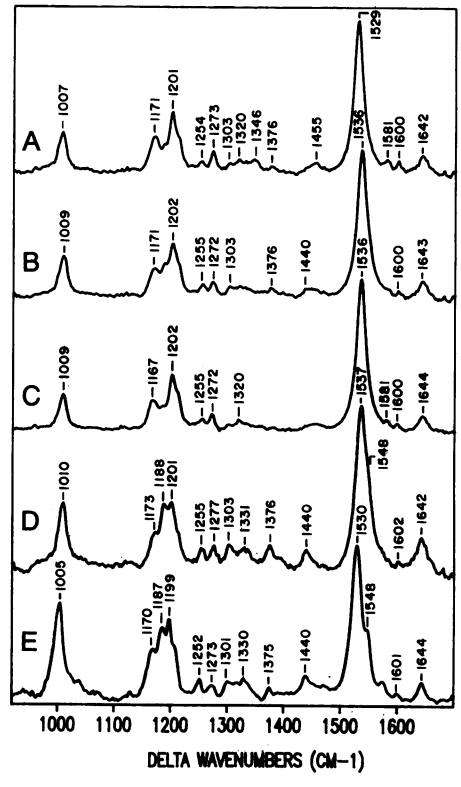

FIG. 5. RR spectra of wild-type bR (*A*) and the L93A mutant (*B*) under continuous illumination (3 mW, 514.5 nm) at pH 6. (*C*) RR spectrum of the L93A mutant recorded with pulsed illumination at pH 6. (*D*) Difference spectrum of the L93A mutant between continuous and pulsed illumination obtained by subtracting the spectrum in *C* from that in *B* such that no negative peaks are generated. (*E*) RR spectrum of the N intermediate of purple membrane obtained by appropriate subtraction (20) of the probe-only spectrum (2 mW, 520.8 nm) of a sample at pH 7 from that of the pump (100 mW, 514.5 nm, 8 ms upstream) and probe (2 mW, 520.8 nm) spectrum of a sample at pH 9 in 3 M KCl/10 mM Tris.

using pulsed illumination with 2-s intervals between successive 100-ms illuminations. Under these conditions, the spectrum should reflect mainly the ground state chromophore, since the photocycle is essentially complete in <2 s (Fig. 4). As expected, this spectrum (Fig. 5*C*) matches the wild-type spectrum shown in Fig. 5*A*. Computation of the difference between spectra recorded under continuous and pulsed illumination (Fig. 5*D*) results in a spectrum that matches that of the N intermediate of the wild-type photocycle (Fig. 5*E*). Significantly, the band at 1005 cm^{-1}, due in part to the rocking vibration of the C-13 methyl group, is shifted to 1010 cm^{-1}. These experiments demonstrate the presence of a long-lived N intermediate in the L93A photocycle. A similar analysis of the RR spectrum of the L93T mutant shows the presence of a long-lived N intermediate in its photocycle (data not shown).

The RR spectra presented here selectively enhance species that are close to the excitation wavelength of 514.5 nm. Thus the contribution of a red-shifted species in the photocycle with a λ_{max} in the vicinity of 595 nm would be relatively weak compared to one with a λ_{max} near 530 nm. Taken together with the data in Fig. 4, we conclude that there exist long-lived N and O species in the photocycle of the L93A mutant and that these may be in equilibrium with each other.

Steady-State Proton Pumping by the Leu-93 Mutants. The steady-state proton transport activities of the L93A, L93T, and L93V mutants are comparable to wild-type bR (Table 3). It is highly significant that the L93A and L93T mutants are as active in steady-state proton transport as wild-type bR given that the lifetimes of the mutant photocycles are increased about 100-fold relative to that of the wild type. These observations suggest that the N and/or O intermediates in the photocycles of the L93A and L93T mutants may be photochemically converted to the ground state to complete a cycle of proton transport. It has been previously suggested that the photoconversion of the N intermediate of the wild-type photocycle to bR is associated with proton uptake from the cytoplasmic medium (3).

DISCUSSION

The most significant findings of the present work are first that Leu-93 interacts with retinal and second that this interaction plays a key role in the photocycle. The lines of evidence leading to these conclusions are as follows: (*i*) The chromophores of the L93A and L93T mutants are blue-shifted

Table 3. Extinction coefficients, steady-state proton pumping, and photocycle parameters for wild-type bR and the Leu-93 mutants at pH 6

Sample	Extinction coefficient,* $M^{-1}\cdot cm^{-1}$	Proton pumping		O decay $t_{1/2}$, ms
		H^+/bR	H^+/bR per s	
Wild type	52,000	31	2.6	5
L93A	49,000	33	2.1	800
L93T	44,000	33	2.7	800
L93V	44,000	40	2.6	5

*Measured at 550 nm for wild-type bR and the L93V mutant and at 530 nm for the L93A and L93T mutants.

with respect to wild-type bR, suggesting possible contact of Leu-93 with retinal. (*ii*) The absorption spectra of the L93A and L93T mutants show little change upon dark adaptation. In wild-type bR, dark adaptation results in a shift of the λ_{max} from ≈560 nm to ≈550 nm, a process that is known to be associated with all-*trans*-retinal → 13-*cis*-retinal isomerization. (*iii*) In contrast to wild-type bR, the retinal isomer composition in the L93A and L93T mutants is predominantly all-trans in both light- and dark-adapted states. (*iv*) The rates of chromophore formation in the L93A and L93T mutants are about 5-fold slower with 13-*cis*-retinal than with the all-trans form, whereas in wild-type bR the rate of formation of the 13-cis chromophore is slightly faster than the all-trans chromophore. This suggests altered affinities in the mutants for 13-*cis*-retinal relative to all-*trans*-retinal during chromophore formation. (*v*) Time-resolved visible absorption spectroscopy shows that the decay of the O intermediate in the photocycles of the L93A and L93T mutants is slowed down by ≈100-fold compared to wild-type bR. (*vi*) RR spectroscopy of the L93A and L93T mutants shows the existence of a long-lived N intermediate in the photocycle, which could be in equilibrium with the O intermediate. (*vii*) Since a >1000-fold increase in bulk proton concentration (from pH 8.5 to pH 5) does not accelerate the decay of the O intermediate, it is clear that the slowest step in the L93A photocycle is uncoupled from proton uptake and reflects the rate of an internal protein structural change. The above observations show that Leu-93 has an important influence on retinal geometry and in the structural changes that occur during the decay of the N and O intermediates.

In principle, at least three changes in conformation may be expected to occur during the photocycle: a first change during the bR → M transition, which results in Schiff base deprotonation and proton release to the external medium; a second change during the decay of the M intermediate, which causes the Schiff base to be reprotonated from the cytoplasmic side rather than the extracellular side; and a third change during the return of the N intermediate to the bR state, which is associated with proton uptake from the cytoplasmic side and the reisomerization of retinal to the all-trans form. Evidence for changes in secondary structure during the bR → M transition comes from spectroscopic (22) and x-ray diffraction (23) studies. Chemical evidence for a conformational change in this step comes from recent studies of the hydroxylamine reactivity of the Schiff base in wild-type bR and selected mutants. These studies indicate that there is a transient increase in water accessibility to the Schiff base before formation of the M intermediate (24). Fourier-transform IR spectroscopy experiments (25) show that the next step of the photocycle (i.e., decay of the M intermediate) also results in a conformational change. Much less is known about the conformational changes that occur during the decay of the N and O intermediates. The present work shows that the replacement of a nonpolar residue in the interior of the protein can greatly influence the rate of structural changes in the final stages of the photocycle.

What is the specific nature of the interaction of Leu-93 with retinal? A possible mechanism for this interaction is suggested by the combined structural evidence from recent cryoelectron microscopic studies (16), by the orientation of the ionone ring of retinal inferred from linear dichroism (26) and neutron diffraction (27) experiments, and by the RR experiments presented here. In a molecular model of bR based on the coordinates provided by R. Henderson *et al.* (16), Leu-93 is seen to be in van der Waals contact with the methyl group on C-13 of retinal. Further, the RR data indicate a shift in the frequency of the methyl rocking vibration at the N stage of the L93A photocycle. The interaction of Leu-93 with the C-13 methyl group could thus be an important element in mediating the coupling between changes in retinal geometry and protein conformation during the photocycle. However, it is also possible that the observed effects of amino acid replacements of Leu-93 are due to the secondary perturbations of other residues in the vicinity of retinal.

The availability of mutants such as L93A and L93T that stabilize the N and O intermediates provides a good opportunity to characterize the latter stages of the photocycle and to address some of the outstanding questions regarding the mechanism of proton transport. For example, does the kinetics of O formation match that of proton uptake from the cytoplasm and the protonation of Asp-96? Is the configuration of retinal in the long-lived O intermediate best described as being in the all-trans, twisted all-trans (28), or 13-cis form? At what stage of the photocycle (N → O or O → bR) does Asp-85 get deprotonated, following its protonation in the L → M transition (11, 12)? What are the factors that influence the rate of 13-cis → all-trans reisomerization? And finally, what are the structural features of the protein conformational change that occurs during the N → bR transition of the photocycle?

We thank Maarten Heyn and Peter Scherrer for suggestions and careful scrutiny of the manuscript, Shankar Subramaniam for helpful discussions, and Stuart Berkowitz for assembling the apparatus for visible spectroscopy. This work was supported by grants from the National Institutes of Health and Office of Naval Research to H.G.K. and by a fellowship from the Damon Runyon–Walter Winchell Cancer Research Fund to S.S.

1. Stoeckenius, W., Lozier, R. H. & Bogomolni, R. A. (1979) *Biochim. Biophys. Acta* **505**, 215–278.
2. Grzesiek, S. & Dencher, N. (1986) *FEBS Lett.* **208**, 337–342.
3. Kouyama, T., Nasuda-Kouyama, A., Ikegami, A., Mathew, M. K. & Stoeckenius, W. (1988) *Biochemistry* **27**, 5855–5863.
4. Otto, H., Marti, T., Holz, M., Mogi, T., Lindau, M., Khorana, H. G. & Heyn, M. P. (1989) *Proc. Natl. Acad. Sci. USA* **86**, 9228–9232.
5. Ames, J. B. & Mathies, R. A. (1990) *Biochemistry* **29**, 7181–7190.
6. Mogi, T., Stern, L. J., Marti, T., Chao, B. H. & Khorana, H. G. (1988) *Proc. Natl. Acad. Sci. USA* **85**, 4148–4152.
7. Butt, H. J., Fendler, K., Bamberg, E., Tittor, J. & Oesterhelt, D. (1989) *EMBO J.* **8**, 1657–1663.
8. Marinetti, T., Subramaniam, S., Mogi, T., Marti, T. & Khorana, H. G. (1989) *Proc. Natl. Acad. Sci. USA* **86**, 529–533.
9. Otto, H., Marti, T., Holz, M., Mogi, T., Stern, L. J., Engel, F., Khorana, H. G. & Heyn, M. P. (1990) *Proc. Natl. Acad. Sci. USA* **87**, 1018–1022.
10. Stern, L. J. & Khorana, H. G. (1989) *J. Biol. Chem.* **264**, 14202–14208.
11. Braiman, M. S., Mogi, T., Marti, T., Stern, L. J., Khorana, H. G. & Rothschild, K. J. (1988) *Biochemistry* **27**, 8516–8520.
12. Gerwert, K., Hess, B., Soppa, J. & Oesterhelt, D. (1989) *Proc. Natl. Acad. Sci. USA* **86**, 4943–4947.
13. Marti, T., Otto, H., Mogi, T., Rösselet, S. J., Heyn, M. P. & Khorana, H. G. (1991) *J. Biol. Chem.* **266**, 6919–6927.
14. Duñach, M., Berkowitz, S., Marti, T., He, Y. W., Subramaniam, S., Khorana, H. G. & Rothschild, K. J. (1990) *J. Biol. Chem.* **265**, 16978–16984.
15. Khorana, H. G. (1988) *J. Biol. Chem.* **263**, 7439–7442.
16. Henderson, R., Baldwin, J. M., Ceska, T. A., Zemlin, F., Beckmann, E. & Downing, K. H. (1990) *J. Mol. Biol.* **213**, 899–929.
17. Fodor, S. P. A., Ames, J. B., Gebhard, R., van den Berg, E. M. M., Stoeckenius, W., Lugtenburg, J. & Mathies, R. (1988) *Biochemistry* **27**, 7097–7101.
18. Argade, P. V. & Rothschild, K. J. (1983) *Biochemistry* **22**, 3460–3466.
19. Varo, G. & Lanyi, J. K. (1991) *Biochemistry* **30**, 5008–5015.
20. Nakagawa, M., Maeda, A., Ogura, T. & Kitagawa, T. (1991) *J. Mol. Struct.* **242**, 221–234.
21. Aton, B., Doukas, A. G., Callender, R. H., Becher, B. & Ebrey, T. G. (1977) *Biochemistry* **16**, 2995–2999.
22. Braiman, M. S., Ahl, P. L. & Rothschild, K. J. (1987) *Proc. Natl. Acad. Sci. USA* **84**, 5221–5225.
23. Koch, M. H. J., Dencher, N. A., Oesterhelt, D., Plöhn, H.-J., Rapp, G. & Buldt, G. (1991) *EMBO J.* **10**, 521–526.
24. Subramaniam, S., Marti, T., Rösselet, S. J., Rothschild, K. J. & Khorana, H. G. (1991) *Proc. Natl. Acad. Sci. USA* **88**, 2583–2587.
25. Braiman, M. S., Bousche, O. & Rothschild, K. J. (1991) *Proc. Natl. Acad. Sci. USA* **88**, 2388–2392.
26. Lin, S. W. & Mathies, R. A. (1989) *Biophys. J.* **56**, 653–660.
27. Hauss, T., Grzsiek, S., Otto, H., Westerhausen, J. & Heyn, M. P. (1990) *Biochemistry* **29**, 4904–4913.
28. Smith, S. O., Pardoen, J. A., Mulder, P. P. J., Curry, B., Lugtenburg, J. & Mathies, R. (1983) *Biochemistry* **22**, 6141–6148.